Published in : European Polymer Journal (2021), vol. 147, n°110296
DOI: 10.1016/j.eurpolymj.2021.110296
Status : Postprint (Author's version)

IMIDAZOLIUM-CATALYZED DYNAMIC ESTER CROSS-LINKS TOWARDS REPROCESSABLE EPOXY VITRIMERS

Panagiotis G. Falireas, Jean-Michel Thomassin, Antoine Debuigne *

Center for Education and Research on Macromolecules (CERM), CESAM Research Unit, University of Liege, Sart-Tilman B6a, 4000 Liege, Belgium
**Corresponding author : E-mail address: adebuigne@uliege.be (A. Debuigne)*

ABSTRACT

Ionic liquids (ILs), in particular imidazolium salts, have raised huge interest as organocatalysts in recent years but have never been considered as activators in associative covalently adaptable networks, also referred to as vitrimers. In this work, we described the first imidazolium-catalyzed vitrimers. The latter consist in epoxy-acid resins that can be reshaped and recycled through catalyzed associative transesterification reactions. A series of cross-linked epoxy-acid networks were produced in the presence of different imidazolium-acetate salts prepared by the straightforward Radziszewski multicomponent reaction. The mechanical properties and dynamics of the resulting materials were studied. Stress-relaxation experiments carried out on resins formulated with few percent of imidazolium salts highlighted the ability of the latter to promote transesterification reactions within the networks and to confer them with vitrimers' features. These imidazolium-catalyzed epoxy vitrimers were also successfully recycled several times while preserving their excellent mechanical properties. Overall, this work demonstrates the potential of ILs as catalysts in the field of adaptable networks and, given the large variety of ILs and of the IL-catalyzed reactions, this approach is likely to broaden the scope of vitrimers in the future.

KEYWORDS: COVALENT ADAPTABLE NETWORKS ; VITRIMERS ; EPOXY-ACID RESIN ; IONIC LIQUIDS ; IMIDAZOLIUM SALT CATALYS

Published in : European Polymer Journal (2021), vol. 147, n°110296
DOI: 10.1016/j.eurpolymj.2021.110296
Status : Postprint (Author's version)

1. Introduction

Epoxy resins constitute an important class of materials on the global thermosetting polymer market. They are used in a plethora of industrial applications demanding superior mechanical properties, chemical inertness, good adhesive properties, etc. Their severe conditions of use are favorable to mechanical damages like cracks and fractures leading to a notable decrease in the lifetime of the networks. A downside of conventional epoxy resins is the impossibility to restore or recycle them by applying heat or by dissolution in solvents due to their permanent cross- linked structure. As a result, incineration and landfill are mainly used for their disposal but both approaches give rise to serious environmental issues, health concerns, safety hazard and wastage of resources. Moreover, the persistent increase in oil prices over the past decades as well as the tendency of national and international political efforts to promote green growth encourage the development of recyclable and healable thermosetting polymer materials.

In this context, the design of covalent adaptable networks (CANs) involving dynamic cross-linking bonds witnessed a considerable growth recently.[1–9] The network rearrangement induced by dynamic exchange reactions provides healing and recycling ability as well as environmental adaptability to these materials. CANs can be classified into two categories based on their exchange reaction mechanism that can be dissociative or associative.[4] In contrast to dissociative CANs relying on temporary rupture of the cross-links, associative CANs, also referred to as vitrimers,[10] maintain a constant cross-linking density during their processing owing to the simultaneous breakage and reformation of the covalent bonds (Fig. 1a). In this dynamic regime, the material flows without structural damage or loss of material properties, remains insoluble and behaves like a viscoelastic melt. At their service temperature, however, vitrimers perform as permanently cross-linked thermosetting materials showing excellent mechanical properties and shape persistence. Several types of covalent exchange reactions have been considered for the preparation of vitrimers including transesterification,[11–14] transcarbamoylation,[15,16] transcarbonation, [17] transamination,[18–21] transalkylation [22,23] leading to a large variety of dynamic networks. Given the importance of epoxy resins, epoxy/acid and epoxy/anhydride vitrimers based on dynamic transesterification reactions have been described early on. [10,13,24–33] In these cases, the exchange process is promoted by catalysts such as zinc carboxylates,[10,26–28] triazobicyclodecenes,[1,25,29] organotin catalysts,[13,30] triphenylphosphine,[32] tertiary amines.[31] Despite the recognized activity of the aforementioned compounds, the search for alternative non-toxic catalysts with higher efficiency, low leaching tendency as well as low moisture, heat or air sensitivity is still relevant.

In recent years, ionic liquids (ILs) have received substantial interest in the scientific community in particular for applications in the field of polymer science.[34–36] They are composed of bulky organic cations associated to a variety of anions and their physical properties can be tuned by a suitable choice of the cation/anion combination. This unique advantage endows ionic liquids with outstanding properties and features such as high chemical and thermal stability, low vapor pressure, high conductivity and the ability to dissolve a wide range of inorganic/ organic

Published in : European Polymer Journal (2021), vol. 147, n°110296
DOI: 10.1016/j.eurpolymj.2021.110296
Status : Postprint (Author's version)

compounds.[37,38] Therefore, ILs sustain, nowadays, countless fields of applications including gas capture,[39–41] electrochemistry, [42,43] and environmentally friendly solvent.[44,45] ILs such as pyridinium, phosphonium, ammonium, sulfonium, and particularly imidazolium salts, were also used as efficient alternative homogeneous catalyst especially in esterification and transesterification reactions. [46–48] For example, imidazolium-based ILs notably catalyze transesterification reactions for biodiesel production.[49] Moreover, imidazolium acetate-based copolymers [50] and networks[51] were also used as supported catalysts in transesterification and decarboxylation reactions.

Driven by the attractive catalytic activity of ILs, we explored the preparation of epoxy-acid resins in the presence of imidazolium compounds for the first time and produced unprecedented imidazolium- catalyzed epoxy vitrimers (Fig. 1b). The latter derived from bisphenol A diglycidyl ether (DGEBA) and adipic acid (AA) cured in the presence of imidazolium acetate derivatives. Two ILs were considered to activate the dynamic transesterification reactions of the resulting networks, namely 1,3-di-butyl-imidazolium acetate ([DiBuIm]+[AcO]-) and 1,3-di- (3-hydroxypropyl)-imidazolium acetate ([DiPrOHIm]+[AcO]-). Structures as well as thermal and mechanical properties of the different resins were studied and discussed. Model reactions were also implemented to gain more insight into the nature of the networks and the impact of imidazolium salts on the course of the curing. Finally, the dynamics of the ester-linked epoxy resins was assessed by stress relaxation experiments and their recycling ability was demonstrated for several cycles.

Fig. 1. *Schematic representation of (a) associative CAN and (b) general strategy for the synthesis of imidazolium-catalyzed epoxy vitrimers.*

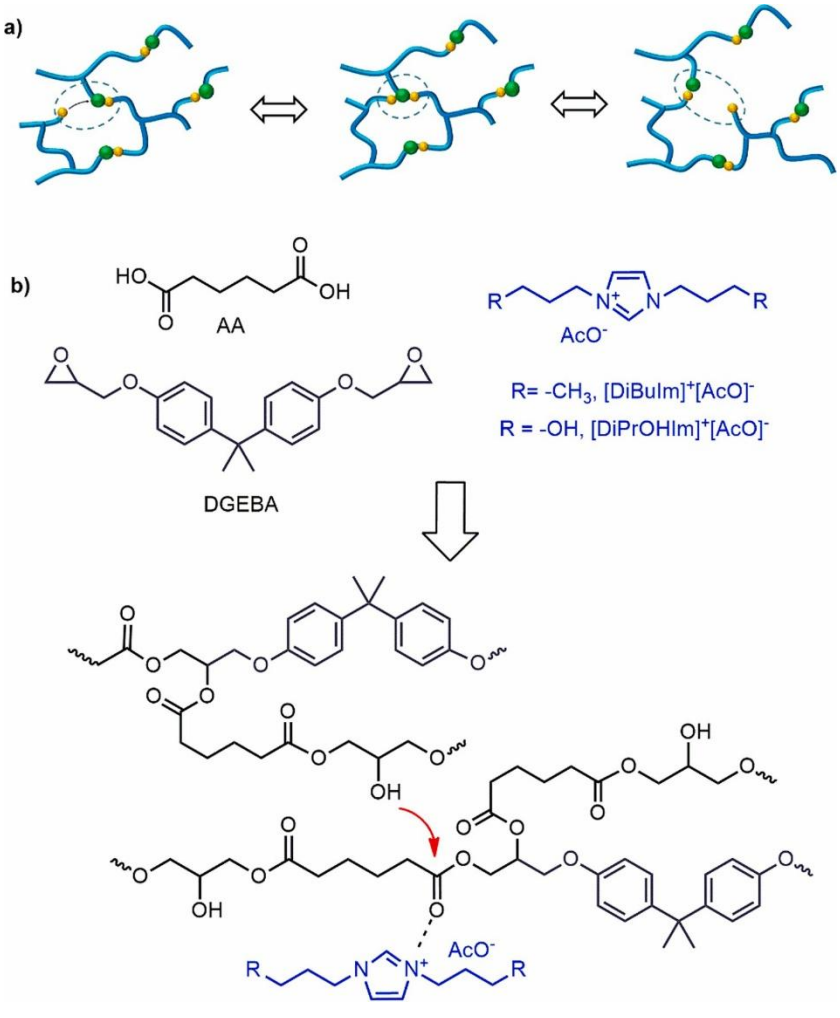

Published in : European Polymer Journal (2021), vol. 147, n°110296
DOI: 10.1016/j.eurpolymj.2021.110296
Status : Postprint (Author's version)

2. Experimental section

2.1. Materials

Diglycidyl ether bisphenol A (DGEBA, >95%), adipic acid (AA, >99%), glycine (>98.5%), butylamine (>99.5%), 3-amino-1-propanol (>99.5%), formaldehyde solution (36.5–38% in H_2O), glyoxal solution (40 wt% in H_2O), vinyl acetate (VAc, >99%), acetic acid (100%), dichloromethane (DCM, ≥99.8%), methanol (MeOH, anhydrous 99.8%), acetonitrile (CH_3CN, anhydrous 99.8%), sodium iodine (NaI, ≥99.5%) 1,2-epoxydodecane (90%) and hexanoic acid (>99%) were purchased from Sigma Aldrich and used as received. Deuterated water (D_2O) and chloroform ($CDCl_3$) (purity > 99.8%) used for ^{1}H and ^{13}C Nuclear Magnetic Resonance spectroscopy were purchased from Euroiso-top (Grenoble, France).

2.2. Characterization

Nuclear Magnetic Resonance (NMR) spectra (^{1}H and ^{13}C) were recorded with a 400 MHz Bruker spectrometer using D_2O or $CDCl_3$ as deuterated solvents and treated with MestreNova software. The sample temperature was set to 298 K. Chemical shifts and coupling constants are given in parts per million (ppm) and Hertz (Hz), respectively.

Fourier Transform Infrared (FTIR) spectra were recorded on a Thermo Fisher Scientific Nicolet IS5 equipped with an ATR ID5 module using a diamond crystal. The spectra were collected in the range (650–4000 cm^{-1}) at a resolution of 4 cm^{-1}.

ESI-MS data were acquired on a Waters Synapt G2-Si mass spectrometer (Waters, UK) equipped with an Electrospray ionization source used in the positive ion mode. Infusion samples were prepared in methanol for the HRMS measurements and acetonitrile for the model reaction investigation. The final concentration of the infused solution is around 1.10–3 mg/mL. For the mass spectrometer parameters, the electrospray ionization (ESI) conditions were capillary voltage 3.1 kV; cone voltage 30 V; source temperature 100 °C; desolvation temperature 150 °C. Dry nitrogen, the desolvation gas, is used as the ESI gas with a flow rate of 500 L h-1 for. For the HRMS (High Resolution Mass Spectrometry – Accurate Mass Measurements) measurements, a solution of NaI is used to prepare reference ions (lock masses).

Thermogravimetric analysis (TGA) analyses were carried out under nitrogen from ambient temperature to 600 °C at a heating rate of 10 °C/ min. Differential scanning calorimetry (DSC) measurements were performed on a TA Instruments Q100 DSC, using hermetic aluminum pans, indium standard for calibration, nitrogen as the purge gas, a sample weight of ~5-10 mg. The measure procedure consisted of two scanning cycles. In each cycle, the sample was cooled down to − 15 °C at a cooling rate of 20 °C/min, followed by an isotherm at − 15 °C for 5 min and heating up to 200 °C at a 10 °C/min heating rate. Glass transition temperatures (T_g) were determined by the inflection point of the curve observed from the second heating cycle.

Published in : European Polymer Journal (2021), vol. 147, n°110296
DOI: 10.1016/j.eurpolymj.2021.110296
Status : Postprint (Author's version)

Dynamic mechanical analysis (DMA) and stress–strain measurements were performed on a DMA Q800 (TA instruments) dynamic mechanical analyzer employing a film tension geometry using rectangular compression-molded films (ca.10.0 mm (L) × 5.0 mm (W) × 1.0 mm (T). Throughout DMA measurements, the storage modulus (E') was monitored as the temperature was increased from 0 °C to 160 °C with a heating rate of 3 °C/min at a frequency of 1 Hz. A preload force of 0.01 N, an amplitude of 5 μm and a force track of 125% were used at all measurements. The T_{alpha} was obtained from the peak temperature of loss tangent (tan δ) curves. Stress–strain curves were performed under the controlled force mode at 25 °C applying a ramp of force from 0 to 18 N with a rate of 0.3 N/min.

Stress relaxation analyses were performed on an ARES-G2 (TA instruments) via parallel plate geometry using disk-shaped specimens of diameter 25 mm and uniform thickness 1–1.5 mm. Prior to measurement, the sample was equilibrated at the selected temperature for 5 min. Strain sweep experiments were carried out for the determination of the linear viscoelastic regime. In all cases, 5% strain step was employed and the stress relaxation behavior was studied in the range from 180 to 240 °C. A constant axial force of 10 N was applied throughout the experiment to maintain the sample between the parallel plates and avoiding sliding. The characteristic relaxation time τ* was determined as the time required to relax to 37% (1/e) of the initial normalized relaxation modulus. Relaxation times τ* follows an Arrhenius law:

$$\tau(T) = \tau_0 \, exp(E_a/RT) \quad (1)$$

where τ_0 refers to the characteristic relaxation time at infinite T, E_a represents the activation energy for the transesterification reaction, R is the universal gas constant and T is the temperature of the conducted experiment.

Swelling tests were carried out with round disc-shaped specimens with an average mass of 600 mg. DCM was used to perform the solubility tests. The specimens were immersed in each solvent for 24 h at 25 °C. Subsequently, the swollen samples were weighted then dried overnight under vacuum at 80 °C to obtain the dry weight. The swelling ratio and soluble fraction were calculated using equation (2) and (3), respectively. The reported results are averages of three measurements.

$$Swelling\ ratio\ (\%) = \frac{m_{swollen} - m_{dry}}{m_{dry}} \times 100 \quad (2)$$

$$Soluble\ fraction\ (\%) = \frac{m_{initial} - m_{dry}}{m_{initial}} \times 100 \quad (3)$$

2.3. Synthesis of 1,3-di-butyl-imidazolium acetate ([DiBuIm]$^+$[AcO]$^-$)

In a 250 mL round-bottom flask equipped with a stirrer bar, a solution of glyoxal (9.92 g, 68 mmol), butylamine (10.00 g, 137 mmol) and formaldehyde (5.54 g, 68 mmol) in MilliQ® water (40 mL) was prepared. Acetic acid (23.48 mL, 410 mmol) was added and the reaction was stirred at 50 °C for 18 h. The reaction mixture was then cooled down to 25 °C and the product was extracted with ethyl acetate (2 × 100 mL). The organic fraction was concentrated under reduced pressure at 80 °C, overnight, to obtain a highly viscous dark-brown liquid (95% yield). ^{1}H NMR (400 MHz, D_2O) δ (ppm)

Published in : European Polymer Journal (2021), vol. 147, n°110296
DOI: 10.1016/j.eurpolymj.2021.110296
Status : Postprint (Author's version)

: 8.77 (s, 1H), 7.47 (s, 2H), 4.16–4.19 (tr, *J* = 7.1 Hz, 4H), 1.95 (s, 3H), 1.81–1.84 (m, 4H), 1.24–1.31 (m, 4H), 0.87–0.89 (tr, *J* = 7.1 Hz, 6H), ^{13}C NMR (101 MHz, D_2O) δ (ppm): 179.67, 135.04, 122.25, 49.24, 31.19, 22.05, 18.70, 12.55. HR-MS *(m/ z)*: $[M]^+$ calcd for $C_{11}H_{21}N_2^+$, 181.1705; found, 181.1705.

2.4. Synthesis of 1,3-di-(3-hydroxypropyl)-imidazolium acetate ($[DiPrOHIm]^+[AcO]^-$)

In a 250 mL round bottom flask containing a stirrer bar, a solution of glyoxal (9.66 g, 67 mmol), 3-amino-1-propanol (10.00 g, 133 mmol) and formaldehyde (5.40 g, 67 mmol) in MilliQ® water (40 mL) was prepared. Acetic acid (22.9 mL, 399 mmol) was added and the reaction was stirred at 50 °C for 18 h. The reaction mixture was then cooled down to 25 °C and the product was extracted with ethyl acetate (2 × 100 mL). The organic fraction was concentrated under reduced pressure at 80 °C overnight to obtain a highly viscous dark-brown liquid (95% yield). ^{1}H NMR (400 MHz, D_2O) δ (ppm): 8.83 (s, 1H), 7.52 (s, 2H), 4.29–4.33 (tr, *J* = 7.1 Hz, 4H), 3.60–3.63 (tr, *J* = 6.1 Hz, 4H), 2.07–2.13 (m, 4H), 1.9 (s, 3H) ^{13}C NMR (101 MHz, D_2O), δ (ppm): 181.02, 135.60, 122.48, 57.85, 46.53, 31.49, 22.96. HR-MS *(m/z)*: $[M]^+$ calcd for $C_9H_{17}N_2O_2^+$, 185.1293; found, 185.1290.

2.5. Synthesis of the epoxy-acid networks

Epoxy vitrimers were synthesized by curing of DGEBA with AA in the presence of $[DiPrOHIm]^+[AcO]^-$ or $[DiBuIm]^+[AcO]^-$. For all samples, an equimolar [COOH]/[epoxy] ratio was used. The experimental procedure carried out in each case is described below. Predetermined amounts of DGEBA and AA were added in a silicone mold (W × D × H = 6 cm × 4 cm × 2 cm) which contained a stirrer bar. A minimum amount of DCM was added and the mixture was dissolved under stirring. Subsequently, an aliquot of $[DiPrOHIm]^+[AcO]^-$ or $[DiBuIm]^+[AcO]^-$ varying from 3 and 5 mol% relative the carboxyl groups was added to the solution and the latter was allowed to stir until a homogeneous mixture was obtained. Subsequently, the mold was placed in an oven at 110 °C for 2 h leading to a homogeneous residue after solvent evaporation. The latter was then cured in the oven at 140 °C for 24 h. Prior removal from the oven, vacuum was applied for 1 h. Finally, the samples were pressed for 90 min at 200 °C applying 3 metric tons pressure in order to obtain transparent and defect free films that were analyzed by IR, TGA, DMA, DSC, stress-relaxation and stress strain experiments.

2.6. Imidazolium catalyzed epoxy-acid model reaction

In a 25 mL round bottom flask equipped with a magnetic stirrer, 1,2- epoxydodecane (3.17 g, 17 mmol), hexanoic acid (2.00 g, 17 mmol) and 1,3-di-butyl-imidazolium acetate (0.15 g, 0.51 mmol, 3 mol%) were mixed and heated at 140 °C for 24 h. The crude reaction mixture was analyzed by IR, NMR and ESI-MS analyses.

Published in : European Polymer Journal (2021), vol. 147, n°110296
DOI: 10.1016/j.eurpolymj.2021.110296
Status : Postprint (Author's version)

2.7. Esterification of $[DiPrOHIm]^+[AcO]^-$ by VAc

In a 50 mL round bottom flask containing a stir bar was added $[DiPrOHIm]^+[AcO]^-$ (1 eq, 0.5 g, 2 mmol) followed by the addition of vinyl acetate (10 eq, 1.8 g, 20 mmol). The reaction mixture was stirred at 80 ° C for 18 h. Finally, the product was dried under vacuum at room temperature overnight. ^{1}H NMR (400 MHz, $CDCl_3$), δ (ppm): 7.93 (s, 1H), 4.43–4.47 (tr, *J* = 7.6 Hz, 4H), 4.14–4.17 (tr, *J* = 6.0 Hz, 4H), 2.20–2.29, (m, 2H) 2.14, (s, 3H) 2.04, 1.80 (s, 3H), 1.78 (s, 3H). ^{13}C NMR (101 MHz, $CDCl_3$) *δ* 170.80, 169.69, 142.10, 123.98, 60.89, 46.39, 29.35, 20.89, 18.73.

Fig. 2. *Preparation of (a) the imidazolium-acetate based catalysts and (b) the corresponding epoxy-acid networks*

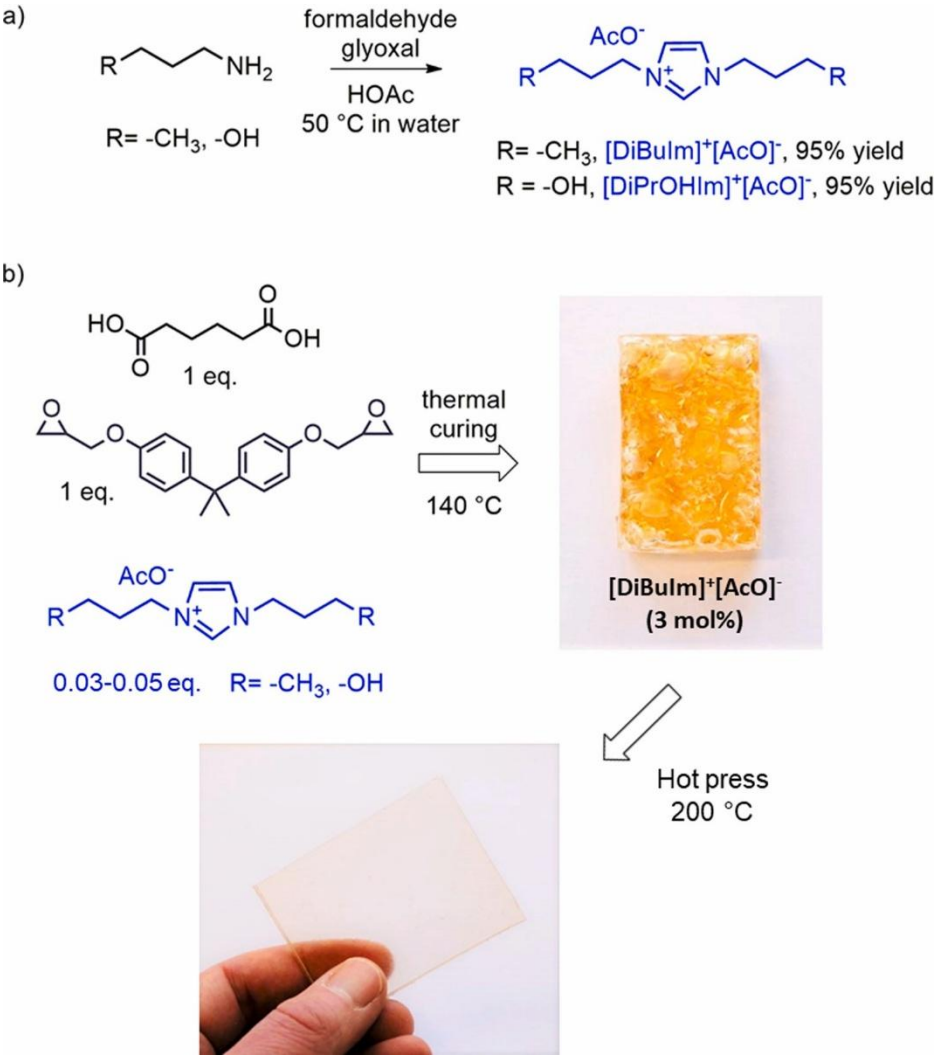

2.8. Recycling experiments

To evaluate the recyclable nature of the networks, samples were ground in small chunks which were then used as a raw material for compression molding. The chunks were placed in metal mold and

Published in : European Polymer Journal (2021), vol. 147, n°110296
DOI: 10.1016/j.eurpolymj.2021.110296
Status : Postprint (Author's version)

pressed at 200 °C for 90 min applying 3 metric tons pressure. This grinding/molding cycle was repeated four times. The resulting homogeneous recycled samples were then cut into rectangular shapes for the tensile experiment.

3. Results and discussion

3.1. Synthesis of the imidazolium acetate catalysts and networks

The imidazolium acetate catalysts were synthesized via the modified Debus-Radziszewski multicomponent reaction (MCR) which consists in coupling two amino groups with glyoxal and formaldehyde in the presence of acetic acid in water.[52] This straightforward one-pot MCR was applied to n-butylamine and 3-amino-1-propanol producing $[DiBuIm]^+[AcO]^-$ and $[DiPrOHIm]^+[AcO]^-$ in 95% yield, respectively (Fig. 2a). These ILs consisting in viscous liquids at room temperature were characterized by ^1H (Figures S1 and S3) and ^{13}C NMR (Figure S2 and S4) to ascertain their chemical structure. The formation of the imidazolium rings was proven by the ^1H signals around 8.7 and 7.5 ppm corresponding to the aromatic protons of the heterocycles and by ^{13}C peaks at 125 and 140 ppm. Characteristic signals of the acetate counter ion were also detected at 1.9 ppm in the ^1H spectra (Figures S1 and S3) and around 177 and 26 ppm in the ^{13}C spectra (Figure S2 and S4). In addition, typical peaks of the terminal methyl groups of $[DiBuIm]^+[AcO]^-$ and of the $–CH_2$-OH methylene groups of $[DiPrOHIm]^+[AcO]^-$ were observed at 0.9 ppm (Figure S1) and 4.3 ppm (Figure S3), respectively.

Next, epoxy-acid networks were synthesized from diglycidyl ether of bisphenol A (DGEBA) and adipic acid (AA) in the presence of various amounts (3 and 5 mol %) of $[DiBuIm]^+[AcO]^-$ or $[DiPrOHIm]^+[AcO]^-$. A stoichiometric amount of diepoxide and diacid was used, which is known to produce crosslinked resins that retain full capacity to flow and relax stresses under thermal treatment.[33] In practice, DGEBA, AA and the imidazolium salts were dissolved in dichloromethane (DCM) and placed in a silicone mold. After evaporation of the solvent at 110 °C, the homogeneous mixture was cured at 140 °C for 24 h. Regardless of the nature ($[DiBuIm]^+[AcO]^-$ or $[DiPrOHIm]^+[AcO]^-$) and the concentration of the imidazolium salts, we recovered stiff and colored materials (Fig. 2b). At this stage, however, the latter exhibited some holes probably due to the release of water leading to bubbles during the curing, as discussed below. Nonetheless, defect free and transparent films were obtained after hot press treatment at 200 °C for 90 min (Fig. 2b) and all analyses have been carried out on these homogeneous materials. Throughout the text, the epoxy-resin (ER) are designated as ER-DiBuIm-n% and ER-DiPrOHIm-n% in reference to the cation and the concentration (n mol%) of catalyst considered in the formulations.

ATR-FTIR analyses were carried out to confirm the formation of the epoxy-acid resins (Figures 3 and S5-6). Representative IR spectra of the DGEBA/AA mixture in the presence of 3 mol% of $[DiBuIm]^+[AcO]^-$ before and after curing at 140 °C and hot press at 200 °C are presented in Fig. 3. First, it is worth noting that spectra for the resins before and after the hot press treatment at 200 °C are very similar. Moreover, upon curing, the characteristic C = O stretching band of the carboxylic acid

Published in : European Polymer Journal (2021), vol. 147, n°110296
DOI: 10.1016/j.eurpolymj.2021.110296
Status : Postprint (Author's version)

at 1680 cm^{-1} disappears while a strong absorption appears at 1730 cm^{-1} due to the formation of the esters (C = O stretching signal) via addition of carboxylic acids onto the epoxy functions of DGEBA (Fig. 3). The consumption of the latter is supported by the disappearance of the characteristic epoxy band at 914 cm^{-1}. Finally, a broad peak emerges around 3100–3600 cm^{-1} which corresponds to the hydroxyl groups generated by the opening of the epoxides (Figures S5A and S6A). Note that some polyether formation, via homopolymerization of the epoxide, is observed in the presence of imidazolium as indicated by the alkyl- alkyl C-O-C signal at 1133 cm^{-1} (Figs. 3 and S5-6). Nevertheless, in the present case, extraction of the specific signal of the epoxy polymerization and accurate quantification of the ether formation is difficult to due to the complexity of the IR pattern in the C-O stretching region (1000–1200 cm^{-1}) and interference with other functions including several ester signals (1280–1160 cm^{-1}), peaks of the aryl–alkyl ether functions (1250 cm^{-1} and 1040 cm^{-1}) as well as primary and secondary alcohol functions (around 1065 cm^{-1} and 1100 cm^{-1}).[33] Interestingly, although part of the epoxy groups are involved in the formation of polyethers, at the term of the reaction, all carboxylic acid groups are consumed. As an explanation, the excess of carboxylic acid reacted by esterification with the alcohol releasing some water at the origin of the holes observed in the cured materials. This situation contrasts with the typical base catalyzed epoxy-acid resin where only two reactions take place, namely the epoxy-acid addition followed by slower transesterification reaction.[53]

In order to gain insight into the network formation, as model reaction, 1,2-epoxydodecane was reacted with hexanoic acid in the presence of 3 mol% of $[DiBuIm]^+[AcO]^-$ at 140 °C. As illustrated in Figure S7, a great variety of products can result from the competing reactions, i.e. opening of the epoxide by the acid, oligomerization of epoxide, esterification of alcohols as well as transesterification. First, the IR analyses confirmed the observations made on the crosslinked materials, i.e. the full consumption of the epoxy and acid groups at the early stage of the reaction (before 3 h), the formation of both ester and ether groups (Figure S8A) as well as significant amount of alcohols (Figure S8B). Further information was provided by ^{1}H NMR (Fig. 4) and HSQC (Figure S9). Aside to the rapid disappearance of epoxy signals (Fig. 4), we observed the appearance of typical signals corresponding to the –COO-C$\underline{H_2}$- of various esters around 3.9–4.2 ppm, the characteristic –C$\underline{H}$-O-C$\underline{H_2}$- peaks of ethers between 3.5 and 3.75 ppm but also the –C$\underline{H}$- OH and –O$\underline{H}$ signals of alcohols around 3.8 and 2.2 ppm, respectively. Interestingly, characteristic –COO-C$\underline{H}$- signals were detected between 4.8 and 5.2 ppm confirming partial esterification of the alcohol released from the opening of the epoxide. Note that some transesterification reactions occurred upon prolonged heating as assessed by the appearance of the additional –COO-C$\underline{H}$- peaks around 4.8–5.2 ppm. Finally, ESI-MS analysis confirmed the complexity of the reaction mixture and the formation of several products (Figure S10). In addition to the imidazolium salt, we identified a series of key products (see blue structures in Figure S7) including the compound resulting from the opening of the epoxy by the acid (A1.Na^+, 323.3 *m*/*z*) and its esterified derivative (A2. Na^+, 421.3 *m*/*z*). Several ether-containing products (e.g. B1, C1-4) resulting from multiple ring opening reactions (with and without esterification of their alcohols) were also detected which supports the occurrence of this reaction during the networks formation.

Published in : European Polymer Journal (2021), vol. 147, n°110296
DOI: 10.1016/j.eurpolymj.2021.110296
Status : Postprint (Author's version)

Finally, the hydroxyl groups of $[DiPrOHIm]^+[AcO]^-$ are likely to react with the precursors of the epoxy-resin but also with the esters of the final material which should lead to the chemical anchoring of the imidazolium onto the network. Due to the low amount of imidazolium involved, it was impossible to highlight this reaction by IR or any other spectroscopic analysis. Therefore, in order to support the ability of the alcohol moieties of $[DiPrOHIm]^+[AcO]^-$ to participate to transesterification reactions, we applied the common vinyl acetate-based transesterification model reaction onto the 1,3-di-(3-hydroxypropyl)- imidazolium acetate. Vinyl acetate (VAc) was selected because the released vinyl alcohol tautomerizes into acetaldehyde, which drives the equilibrium towards the product side and facilitates the analysis of the esterified compound.[54] In practice, $[DiPrOHIm]^+[AcO]^-$ was reacted with 10 equivalents of VAc at 80 °C for 18 h (Figure S11a). Under these conditions, the corresponding esterified imidazolium salt was produced near-quantitatively, according to ^1H and ^{13}C NMR (Figures S11b and S11c), highlighting the propensity of its hydroxyl groups to take part to transesterification processes.

Overall, the characterization of the epoxy resins prepared with the imidazolium salts confirmed the proper cross-linking reaction as well as the formation of both ester and alcohol moieties necessary to the transesterification exchange reactions behind the vitrimer-like properties. The latter are studied below.

Fig. 3. *ATR-FTIR spectra of the starting DGEBA/AA mixture (—) and of the resulting ER-DiBuIm-3% after curing at 140 ◦C (—) and hot press at 200 ◦C (—). Peaks labels: (A) C =O stretching of adipic acid, (B) asymmetric epoxy deformation, (C) C =O stretching of esters of the network, (D) C-O-C peaks of ethers.*

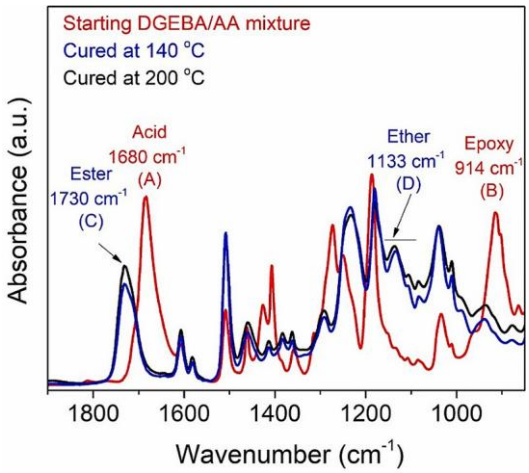

Published in : European Polymer Journal (2021), vol. 147, n°110296
DOI: 10.1016/j.eurpolymj.2021.110296
Status : Postprint (Author's version)

***Fig. 4**. ^{1}H NMR (in $CDCl_3$) of the model reaction between 1,2-epoxydodecane and hexanoic acid carried out at 140 °C in the presence of 3 mol % of $[DiBuIm]^+[AcO]^-$.*

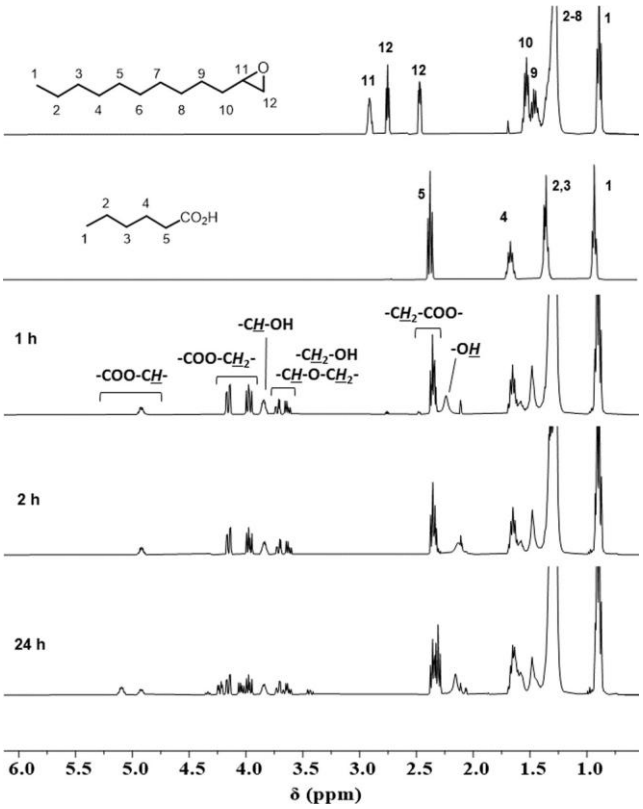

***Table 1** Swelling ratio and soluble fraction of the epoxy resins.*

Sample	Swelling ratio (%) [a]	Soluble fraction (%) [b]
ER-DiBuIm-3%	129	6
ER-DiBuIm-5%	166	7
ER-DiPrOHIm-3%	147	5
ER-DiPrOHIm-5%	154	8

Analyses were carried on the samples cured at 140 °C and pressed at 200 °C. [a] Determined after 24 h immersion in DCM according to eq. (2). [b] Determined from the weight loss of the sample according to eq. (3).

3.2. Network characterization

Swelling experiments were first carried out to assess the covalent cross-linked character and the solvent resistance of the materials (Table 1). For this purpose, the epoxy-acid samples were immersed for 24 h in DCM at ambient temperature. In all cases, swelling ratios ranging from about 130 to 165% and low soluble fractions (<8%) were recorded. In spite of the good affinity of the solvent for these polymers, the latter did not dissolve (even after a prolonged immersion of two weeks) which supports their cross-linked nature. The comparable swelling data between the different samples also support the limited impact of the imidazolium catalyst on the material microstructure obtained after curing the epoxy and acid precursors, as already evidenced above by IR spectroscopy.

Published in : European Polymer Journal (2021), vol. 147, n°110296
DOI: 10.1016/j.eurpolymj.2021.110296
Status : Postprint (Author's version)

The thermal stability of the different networks was evaluated by thermogravimetric analysis (Figure S12). In particular, we measured the onset degradation temperature $T_{d5\%}$ corresponding to the temperature at which a weight loss of 5% is observed (Table 2). This analysis emphasized the good thermal stability of all materials with $T_{d5\%}$ superior to 300 °C confirming that imidazolium does not favour the thermal degradation of the epoxy-resin.

Next, T_g of each epoxy-resin were measured by DSC (Figure S13, Table 2). In all cases, T_g was comprised between 37 and 47 °C. No drastic change of T_g was observed when the loading of $[DiPrOHIm]^+[AcO]^-$ or $[DiBuIm]^+[AcO]^-$ increased. As a confirmation, very similar T_{alpha} values were measured by DMA for the different samples (Figure S14, Table 2). These values are consistent with the previously reported T_g of DGEBA-based vitrimers ranging from 30 °C to 60 °C depending on the length of the diacid derivative (C10-C5).[24]

The viscoelastic properties of the imidazolium-loaded networks were then characterized using DMA. Fig. 5 presents the storage modulus (E') as a function of temperature. All curves displayed characteristic features of crosslinked materials. As expected for epoxy-acid resins in the glassy state,[24,55] the E' values recorded at 25 °C were in the range of GPa (See Fig. 5 and Table 2). Upon heating, the storage modulus exhibited a steep drop when the temperature reaches ~ 50 °C typical of the transition from glassy to rubbery state, followed by a rubbery plateau above 110 °C confirming the presence of a three-dimensional network. On the other hand, the rubbery E' modulus at 150 °C slightly decreases when increasing the amount of catalyst in the formulation, e.g. 1.28 MPa and 0.83 MPa for 3 mol% and 5 mol% of $[DiBuIm]^+[AcO]^-$, respectively. The same trend was observed for $[DiPrOHIm]^+[AcO]^-$ (Table 2). These observations suggest a slightly lower cross-linking density within materials formulated with a higher amount of catalyst, which may be due to minor variations in the ester/ether ratio in the epoxy resins.

The mechanical properties of the $[DiBuIm]^+[AcO]^-$ and $[DiPrOHIm]^+[AcO]^-$ loaded networks were then assessed by stress–strain experiments (Fig. 6, Table 2). The tensile modulus of these materials tends to decrease when increasing the imidazolium content. Indeed, modulus values of 1010 MPa and 650 MPa were recorded for epoxy resins prepared with 3 mol% and 5 mol% of $[DiBuIm]^+[AcO]^-$, respectively. This trend is consistent with the variation in the crosslinking density suggested by the above mentioned evolution of E' in the rubbery plateau. Very similar trends were observed for the epoxy resins formulated with $[DiPrOHIm]^+[AcO]^-$ (Fig. 6).

Table 2 *Thermal and mechanical properties of the epoxy-acid resins*

Sample	Td 5% (°C)a	Tg DSC (°C)b	T alpha (°C)c	E' at 25°C (GPa)[d]	E' at 150 °C (MPa)[d]	Tensile Modulus (MPa)[e]	Ea (kJ/mol)[f]
ER-DiBuIm-3%	356	47	49	3.78	1.28	1010	94
ER-DiBuIm-5%	343	42	50	1.64	0.83	650	110
ER-DiPrOHIm-3%	355	37	49	2.84	1.16	870	71
ER-DiPrOHIm-5%	348	38	50	3.00	0.64	670	75

All analyses were carried on samples cured at 140 °C and pressed at 200 °C.[a] Temperature at which a weight loss of 5% is observed by TGA. [b] Determined by DSC. [c] Determined by DMA (see Figure S14). [d] Storage modulus measured by DMA. [e] Tensile modulus determined at 25 ◦C from stress-strain curves (Fig. 6). [f] Activation energy calculated from the Arrhenius law (data in Fig. 7).

Published in : European Polymer Journal (2021), vol. 147, n°110296
DOI: 10.1016/j.eurpolymj.2021.110296
Status : Postprint (Author's version)

Fig. 5. *Temperature dependence of the storage modulus for epoxy-acid networks formulated with various amounts of (a) [DiBuIm]⁺[AcO]⁻ and (b) [DiPrOHIm]⁺[AcO]⁻.*

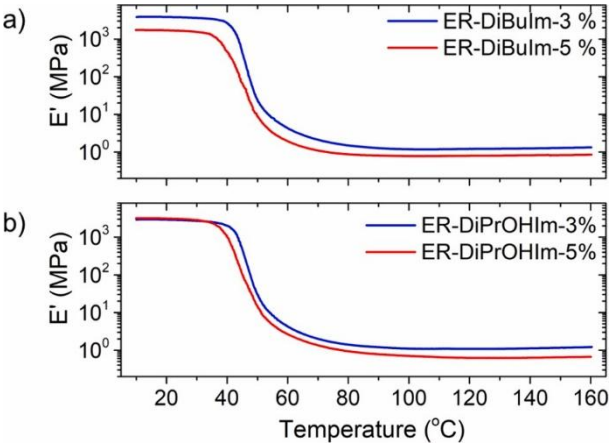

Fig. 6. *Stress–strain curves for epoxy-acid resins (cured at 140 °C and pressed at 200 °C) containing various amounts of a) [DiBuIm]⁺[AcO]⁻ and b) [DiPrOHIm]⁺[AcO]⁻.*

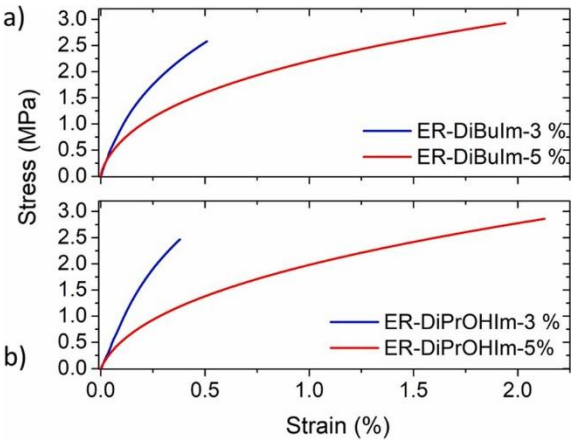

3.3. Networks dynamics

The vitrimer-like properties of the imidazolium-containing epoxy- acid networks were then studied via stress relaxation experiments. In this case, the imidazolium additives are expected to catalyze the transesterification reactions allowing the rearrangement of the ester cross- links and the relaxation of the networks. The effect of the nature and concentration of the imidazolium derivatives on the network dynamics was examined at different temperatures. Shear stress relaxation experiments were performed on epoxy-acid resins containing 3 mol% and 5 mol% of [DiBuIm]⁺[AcO]⁻ or [DiPrOHIm]⁺[AcO]⁻ at various temperatures ranging between 200 °C and 240 °C (Fig. 7). The normalized stress- relaxation curves of all samples at each temperature are provided in Figure S15. As an illustration, Fig. 7a and 7b show representative stress relaxation curves at 200 °C for an applied strain of 5% for networks containing different amounts of [DiBuIm]⁺[AcO]⁻ and [DiPrOHIm]⁺[AcO]⁻, respectively.

Published in : European Polymer Journal (2021), vol. 147, n°110296
DOI: 10.1016/j.eurpolymj.2021.110296
Status : Postprint (Author's version)

As expected, the epoxy-acid resins formulated in the presence of imidazolium exhibited some relaxation at 200 °C and this phenomenon was faster when the imidazolium loading was increased. These observations confirmed the ability of the imidazolium-acetate compounds to play the role of transesterification catalyst and activate the exchangeable ester cross-links. According to previous report, relaxation times τ^* were measured from the stress-relaxation curves and correspond to the time necessary to release 63% of the stress (Table S1). At 200 °C, the relaxation time τ^* of the networks containing between 3 and 5 mol% of $[DiBuIm]^+[AcO]^-$ were equal to 80 min to 55 min, respectively (Table S1). At the same temperature and for an identical catalyst loading, τ^* varied from 85 min to 29 min when using 3 and 5 mol% of $[DiPrOHIm]^+[AcO]^-$, respectively (Table S1). By comparison, these τ^* values are higher than those reported for epoxy-acid vitrimers with comparable glass transition temperatures prepared with the common $Zn(OAc)_2$ catalyst.[32] Indeed, relaxation times of approximately 10 min were measured at 200 °C for such resins containing 5 mol% of $Zn(OAc)_2$.[32] Nevertheless, as shown in Fig. 2, proper reshaping of the imidazolium- based vitrimers can be achieved at 200 °C when the processing time (90 min) exceeds the relaxation time. As shown in Fig. 7c and 7d, the relationship between relaxation time and temperature satisfied the Arrhenius law allowing the calculation of the E_a from the slope. Overall, slightly higher E_as were recorded for the networks loaded with $[DiBuIm]^+[AcO]^-$ (94–110 kJ/mol) compared to those containing $[DiPrOHIm]^+[AcO]^-$ (71–75 kJ/mol) (Table 2). These activation energies are in the range of those reported for several epoxy-acid vitrimers. [10,24,31,55–57] For example, activation energies around 90 kJ/mol were measured for $Zn(OAc)_2$-catalyzed epoxy-acid vitrimers.[32]

Fig. 7. *Normalized stress-relaxation curves for the epoxy-acid resins (cured at 140 °C and pressed at 200 °C) containing different amounts of (a) $[DiBuIm]^+[AcO]^-$ and (b) $[DiPrOHIm]^+[AcO]^-$ at 200 °C. Relaxations times (τ^*) were measured at 63% of relaxation (dotted line); Arrhenius plots of the measured relaxation times for different loadings of c) $[DiBuIm]^+[AcO]^-$ and d) $[DiPrOHIm]^+[AcO]^-$.*

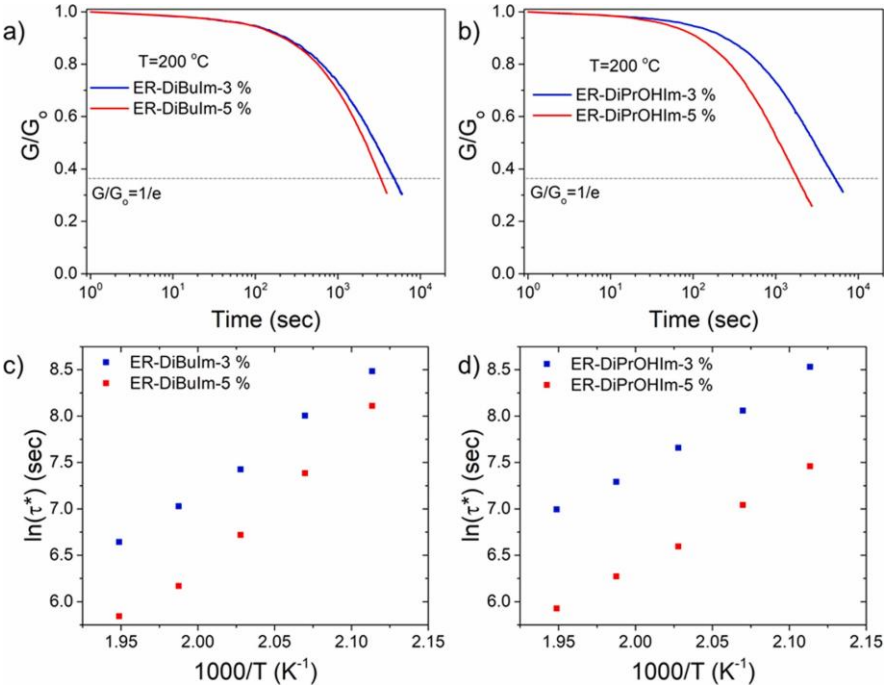

Published in : European Polymer Journal (2021), vol. 147, n°110296
DOI: 10.1016/j.eurpolymj.2021.110296
Status : Postprint (Author's version)

3.4. Recyclability of the networks

The recycling of the imidazolium catalyzed epoxy-acid resins was also addressed. In this case, we considered networks containing 3 mol% of catalyst, i.e. $[DiBuIm]^+[AcO]^-$ or $[DiPrOHIm]^+[AcO]^-$. For this purpose, samples were crushed in very small pieces and remolded by compression into films at 200 °C by applying 3 metric tons pressure for 90 min. This procedure was repeated four times using the same conditions and stress–strain curves were measured at ambient temperature after each recycling step (Fig. 8a and b). Regardless of the nature of the catalyst, no significant loss of the mechanical properties of the networks was observed after repeated recycling which demonstrates the recyclability of these unprecedented imidazolium-catalyzed epoxy vitrimers. It also is worth remembering at this stage that a model reaction emphasized the propensity of the alcohols of $[DiPrOHIm]^+[AcO]^-$ to undergo transesterification, and so to possibly anchor the ester-based networks. Nevertheless, this phenomenon does not prevent this imidazolium moiety to act as catalyst and to promote an efficient recycling of the resins.

Finally, swelling and DMA analyses were performed on the recycled imidazolium-containing networks to better evaluate the integrity of the network along the recycling steps. As indicated in Table S2, swelling ratios remained in the same range as the original material but slightly decreased along the recycling steps for both $[DiBuIm]^+[OAc]^-$ and $[DiPrOHIm]^+[OAc]^-$ catalysts suggesting that the crosslinking density somewhat increased. This assumption is supported by the moderate increase (log scale) of the E' value in the rubbery plateau of DMA curves of the recycled imidazolium containing networks, as illustrated in Figure S16 for the $[DiPrOHIm]^+[OAc]^-$ based vitrimers. The repetition of the recycling process thus seems to induce some extra crosslinking within the imidazolium-based materials probably due to the high temperature (200 °C) and time necessary for their reprocessing. In spite of this, the recycling of these imidazolium-catalyzed vitrimers is quite effective and the mechanical properties of the materials seem preserved along the recycling steps.

Published in : European Polymer Journal (2021), vol. 147, n°110296
DOI: 10.1016/j.eurpolymj.2021.110296
Status : Postprint (Author's version)

Fig. 8. *Stress-strain curves of recycled imidazolium-loaded vitrimers after grinding to a powder and reprocessing at 200 °C for 90 min. (a) ER-DiBuIm-3% (b) ER-DiPrOHIm-3%.*

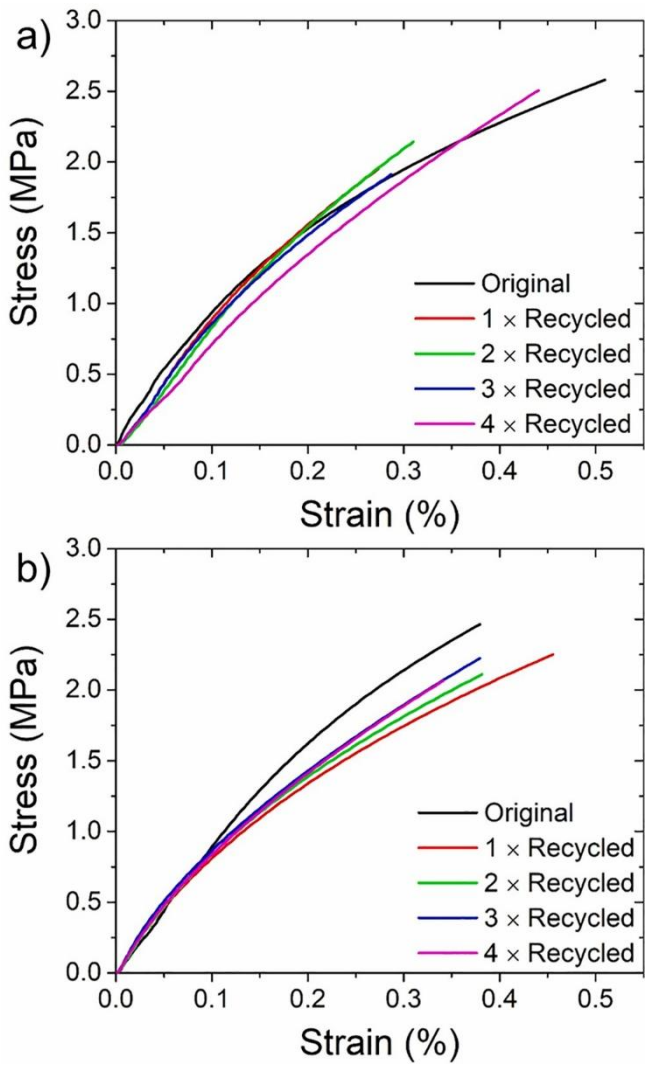

4. Conclusions

In summary, we demonstrated for the first time the potential of imidazolium salts as catalysts for the transesterification covalent exchanges occurring in epoxy-acid vitrimers. A series of resins were formulated from the bisphenol A diglycidyl ether/adipic acid pair in the presence of different amounts of $[DiBuIm]^+[AcO]^-$ or $[DiPrOHIm]^+[AcO]^-$ derivatives. Characterization of the resulting materials confirmed their crosslinked nature as well as the presence of ester and alcohol moieties involved in the dynamic transesterification process. Structural characterizations and model reactions also highlighted the occurrence of the competing ring opening oligomerization of epoxide under these conditions leading to polyether groups inside the network. Nonetheless, these unprecedented imidazolium-containing epoxy-acid resins displayed the characteristic behaviors of vitrimers during the stress-relaxation experiments. Moreover, Arrhenius activation energies and

Published in : European Polymer Journal (2021), vol. 147, n°110296
DOI: 10.1016/j.eurpolymj.2021.110296
Status : Postprint (Author's version)

relaxation times were measured for networks containing various amounts of these catalysts. Briefly, slightly higher E_as were recorded for the networks loaded with $[DiBuIm]^+[AcO]^-$ compared to those containing $[DiPrOHIm]^+[AcO]^-$ and, as expected, relaxation times decreased when increasing the catalyst loading. By comparison, however, relaxation times of these imidazolium vitrimers were higher compared to those involving more common catalysts like $Zn(OAc)_2$ meaning that the former necessitate higher temperature and/or longer processing times.

Despite of this, the imidazolium-containing resins showed good recyclability and reshaping properties which confirms the capacity of imidazolium salts to activate the transesterification reactions responsible for the network's dynamics. Indeed, some resins were recycled>4 times without significant alteration of their mechanical properties.

Considering the relaxation times and the competing polymerization of epoxides during the formation of the imidazolium-based vitrimers, we must concede that the latter does not totally compete with the traditional catalysts like $Zn(OAc)_2$ for the preparation of epoxy-acid vitrimers. Nevertheless, this work demonstrates for the first time the ability of ionic liquid, in particular of imidazolium salts, to act as catalysts in the field of the epoxy-acid adaptable networks. It also sheds light on the fact that the presence of a few percent of imidazolium groups in ester networks is likely to impact their properties and induce some relaxation. Finally, considering the great variety of ILs and the large range of reactions they can catalyze, it should be possible to extend this approach to adaptable networks governed by other types of exchangeable crosslinks and so broaden the scope of vitrimers.

Published in : European Polymer Journal (2021), vol. 147, n°110296
DOI: 10.1016/j.eurpolymj.2021.110296
Status : Postprint (Author's version)

CRediT authorship contribution statement

Panagiotis G. Falireas: Conceptualization, Validation, Investigation, Writing - original draft, Writing - review & editing. **Jean-Michel Thomassin:** Conceptualization, Investigation, Writing - review & editing. **Antoine Debuigne:** Conceptualization, Visualization, Writing - original draft, Writing - review & editing, Supervision, Project administration, Funding acquisition.

Declaration of Competing Interest

The authors declare that they have no known competing financial interests or personal relationships that could have appeared to influence the work reported in this paper.

Acknowledgements

The authors thank the Fonds de la Recherche Scientifique (FNRS) for funding the PDR research project VITRIPILS (ID 9236). A.D. is Senior Research Associate FRS.-FNRS. The authors are also thankful to J. De Winter and P. Gerbaux (UMons) for the MS analyses as well as L. Collard and B. Evrard (ULiege) for the DSC analyses.

Data availability

Additional data are provided in the supporting information section including NMR, DMA, IR, TGA, DSC, rheological analyses. The raw/ processed data required to reproduce these findings cannot be shared at this time due to technical or time limitations.

Appendix A. Supplementary data

Supplementary data to this article can be found online at

https://doi. org/10.1016/j.eurpolymj.2021.110296.

Published in : European Polymer Journal (2021), vol. 147, n°110296
DOI: 10.1016/j.eurpolymj.2021.110296
Status : Postprint (Author's version)

References

[1] C.J. Kloxin, T.F. Scott, B.J. Adzima, C.N. Bowman, Covalent Adaptable Networks (CANs): A Unique Paradigm in Cross-Linked Polymers, Macromolecules 43 (6) (2010) 2643–2653.

[2] C.J. Kloxin, C.N. Bowman, Covalent adaptable networks: smart, reconfigurable and responsive network systems, Chem. Soc. Rev. 42 (17) (2013) 7161–7173.

[3] S. Ji, W. Cao, Y. Yu, H. Xu, Dynamic Diselenide Bonds: Exchange Reaction Induced by Visible Light without Catalysis, Angew. Chem. Int. Ed. 53 (26) (2014) 6781–6785.

[4] W. Denissen, J.M. Winne, F.E. Du Prez, Vitrimers: permanent organic networks with glass-like fluidity, Chem. Soc. Rev. 7 (1) (2016) 30–38.

[5] M. Guerre, C. Taplan, J.M. Winne, F.E. Du Prez, Vitrimers: directing chemical reactivity to control material properties, Chem. Soc. Rev. 11 (19) (2020) 4855–4870.

[6] G.M. Scheutz, J.J. Lessard, M.B. Sims, B.S. Sumerlin, Adaptable Crosslinks in Polymeric Materials: Resolving the Intersection of Thermoplastics and Thermosets, J. Am. Chem. Soc. 141 (41) (2019) 16181–16196.

[7] Y. Jin, Z. Lei, P. Taynton, S. Huang, W. Zhang, Malleable and Recyclable Thermosets: The Next Generation of Plastics, Matter 1 (6) (2019) 1456–1493.

[8] B.R. Elling, W.R. Dichtel, Reprocessable Cross-Linked Polymer Networks: Are Associative Exchange Mechanisms Desirable? ACS Cent. Sci. 6 (9) (2020) 1488–1496.

[9] Jourdain, R. Asbai, O. Anaya, M.M. Chehimi, E. Drockenmuller, D. Montarnal, Rheological Properties of Covalent Adaptable Networks with 1,2,3-Triazolium Cross-Links: The Missing Link between Vitrimers and Dissociative Networks, Macromolecules 53 (6) (2020) 1884–1900.

[10] D. Montarnal, M. Capelot, F. Tournilhac, L. Leibler, Silica-Like Malleable Materials from Permanent Organic Networks, Science 334 (6058) (2011) 965–968.

[11] M. Capelot, D. Montarnal, F. Tournilhac, L. Leibler, Metal-Catalyzed Transesterification for Healing and Assembling of Thermosets, J. Am. Chem. Soc. 134 (18) (2012) 7664–7667.

[12] Legrand, C. Soulié-Ziakovic, Silica-Epoxy Vitrimer Nanocomposites, Macromolecules 49 (16) (2016) 5893–5902.

[13] J.P. Brutman, P.A. Delgado, M.A. Hillmyer, Polylactide Vitrimers, ACS Macro Lett. 3 (7) (2014) 607–610.

[14] Y. Zhou, R. Groote, J.G.P. Goossens, R.P. Sijbesma, J.P.A. Heuts, Tuning PBT vitrimer properties by controlling the dynamics of the adaptable network, Polym. Chem. 10 (1) (2019) 136–144.

[15] N. Zheng, Z. Fang, W. Zou, Q. Zhao, T. Xie, Thermoset Shape-Memory Polyurethane with Intrinsic Plasticity Enabled by Transcarbamoylation, Angew. Chem. Int. Ed. 55 (38) (2016) 11421–11425.

[16] D.J. Fortman, J.P. Brutman, C.J. Cramer, M.A. Hillmyer, W.R. Dichtel, Mechanically Activated, Catalyst-Free Polyhydroxyurethane Vitrimers, J. Am. Chem. Soc. 137 (44) (2015) 14019–14022.

[17] R.L. Snyder, D.J. Fortman, G.X. De Hoe, M.A. Hillmyer, W.R. Dichtel, Reprocessable Acid-Degradable Polycarbonate Vitrimers, Macromolecules 51 (2) (2018) 389–397.

Published in : European Polymer Journal (2021), vol. 147, n°110296
DOI: 10.1016/j.eurpolymj.2021.110296
Status : Postprint (Author's version)

[18] W. Denissen, G. Rivero, R. Nicolaÿ, L. Leibler, J.M. Winne, F.E. Du Prez, Vinylogous Urethane Vitrimers, Adv. Funct. Mater. 25 (16) (2015) 2451–2457.

[19] W. Denissen, M. Droesbeke, R. Nicolaÿ, L. Leibler, J.M. Winne, F.E. Du Prez, Chemical control of the viscoelastic properties of vinylogous urethane vitrimers, Nat. Commun. 8 (1) (2017) 14857.

[20] J.J. Lessard, L.F. Garcia, C.P. Easterling, M.B. Sims, K.C. Bentz, S. Arencibia, D. A. Savin, B.S. Sumerlin, Catalyst-Free Vitrimers from Vinyl Polymers, Macromolecules 52 (5) (2019) 2105–2111.

[21] J.J. Lessard, G.M. Scheutz, S.H. Sung, K.A. Lantz, T.H. Epps, B.S. Sumerlin, Block Copolymer Vitrimers, J. Am. Chem. Soc. 142 (1) (2020) 283–289.

[22] M.M. Obadia, B.P. Mudraboyina, A. Serghei, D. Montarnal, E. Drockenmuller, Reprocessing and Recycling of Highly Cross-Linked Ion-Conducting Networks through Transalkylation Exchanges of C-N Bonds, J. Am. Chem. Soc. 137 (18) (2015) 6078–6083.

[23] B. Hendriks, J. Waelkens, J.M. Winne, F.E. Du Prez, Poly(thioether) Vitrimers via Transalkylation of Trialkylsulfonium Salts, ACS Macro Lett. 6 (9) (2017) 930–934.

[24] F.I. Altuna, C.E. Hoppe, R.J.J. Williams, Shape memory epoxy vitrimers based on DGEBA crosslinked with dicarboxylic acids and their blends with citric acid, RSC Adv. 6 (91) (2016) 88647–88655.

[25] Z. Pei, Y. Yang, Q. Chen, E.M. Terentjev, Y. Wei, Y. Ji, Mouldable liquid-crystalline elastomer actuators with exchangeable covalent bonds, Nat. Mater. 13 (1) (2014) 36–41.

[26] Z. Feng, J. Hu, H. Zuo, N. Ning, L. Zhang, B. Yu, M. Tian, Photothermal-Induced Self-Healable and Reconfigurable Shape Memory Bio-Based Elastomer with Recyclable Ability, Appl. Mater. Interfaces 11 (1) (2019) 1469–1479.

[27] M. Hayashi, R. Yano, A. Takasu, Synthesis of amorphous low Tg polyesters with multiple COOH side groups and their utilization for elastomeric vitrimers based on post-polymerization cross-linking, Polym. Chem. 10 (16) (2019) 2047–2056.

[28] T. Liu, C. Hao, L. Wang, Y. Li, W. Liu, J. Xin, J. Zhang, Eugenol-Derived Biobased Epoxy: Shape Memory, Repairing, and Recyclability, Macromolecules 50 (21) (2017) 8588–8597.

[29] Y. Liu, Z. Tang, S. Wu, B. Guo, Integrating Sacrificial Bonds into Dynamic Covalent Networks toward Mechanically Robust and Malleable Elastomers, ACS Macro Lett. 8 (2) (2019) 193–199.

[30] W. Liu, D.F. Schmidt, E. Reynaud, Catalyst Selection, Creep, and Stress Relaxation in High-Performance Epoxy Vitrimers, Ind. Eng. Chem. Res. 56 (10) (2017) 2667–2672.

[31] F.I. Altuna, C.E. Hoppe, R.J.J. Williams, Epoxy vitrimers with a covalently bonded tertiary amine as catalyst of the transesterification reaction, Eur. Polym. J. 113 (2019) 297–304.

[32] M. Capelot, M.M. Unterlass, F. Tournilhac, L. Leibler, Catalytic Control of the Vitrimer Glass Transition, ACS Macro Lett. 1 (7) (2012) 789–792.

[33] Q.-A. Poutrel, J.J. Blaker, C. Soutis, F. Tournilhac, M. Gresil, Dicarboxylic acid- epoxy vitrimers: influence of the off-stoichiometric acid content on cure reactions and thermo-mechanical properties, Polym. Chem. 11 (33) (2020) 5327–5338.

[34] D. Mecerreyes, Applications of ionic liquids in polymer science and technology, 1 ed., Springer-Verlag, Berlin Heidelberg, 2015.

Published in : European Polymer Journal (2021), vol. 147, n°110296
DOI: 10.1016/j.eurpolymj.2021.110296
Status : Postprint (Author's version)

[35] D. Mecerreyes, Polymeric ionic liquids: Broadening the properties and applications of polyelectrolytes, Prog. Polym. Sci. 36 (12) (2011) 1629–1648.

[36] J. Lu, F. Yan, J. Texter, Advanced applications of ionic liquids in polymer science, Prog. Polym. Sci. 34 (5) (2009) 431–448.

[37] M. Armand, F. Endres, D.R. MacFarlane, H. Ohno, B. Scrosati, Ionic-liquid materials for the electrochemical challenges of the future, Nat. Mater. 8 (8) (2009) 621–629.

[38] C.-Z. Liu, F. Wang, A.R. Stiles, C. Guo, Ionic liquids for biofuel production: Opportunities and challenges, Appl. Energy 92 (2012) 406–414.

[39] A. Dani, V. Crocella, C. Magistris, V. Santoro, J. Yuan, S. Bordiga, Click-based` porous cationic polymers for enhanced carbon dioxide capture, J. Mater. Chem. 5 (1) (2017) 372–383.

[40] S. Soll, Q. Zhao, J. Weber, J. Yuan, Activated CO2 Sorption in Mesoporous Imidazolium-Type Poly(ionic liquid)-Based Polyampholytes, Chem. Mater. 25 (15) (2013) 3003–3010.

[41] Wilke, J. Yuan, M. Antonietti, J. Weber, Enhanced Carbon Dioxide Adsorption by a Mesoporous Poly(ionic liquid), ACS Macro Lett. 1 (8) (2012) 1028–1031.

[42] A.E. Visser, R.P. Swatloski, W.M. Reichert, R. Mayton, S. Sheff, A. Wierzbicki, J. H. Davis Jr., R.D. Rogers, Task-specific ionic liquids for the extraction of metal ions from aqueous solutions, Chem. Commun. 1 (2001) 135–136.

[43] A.E. Visser, R.P. Swatloski, W.M. Reichert, S.T. Griffin, R.D. Rogers, Traditional extractants in nontraditional solvents: Groups 1 and 2 extraction by crown ethers in room-temperature ionic liquids, Ind. Eng. Chem. Res. 39 (10) (2000) 3596–3604.

[44] J.S. Wilkes, Properties of ionic liquid solvents for catalysis, J. Mol. Catal. A: Chem. 214 (1) (2004) 11–17.

[45] C. Chiappe, D. Pieraccini, Ionic liquids: solvent properties and organic reactivity, J. Phys. Org. Chem. 18 (4) (2005) 275–297.

[46] A.S. Amarasekara, Acidic Ionic Liquids, Chem. Rev. 116 (10) (2016) 6133–6183.

[47] M. Selva, A. Perosa, S. Guidi, L. Cattelan, Ionic liquids as transesterification catalysts: applications for the synthesis of linear and cyclic organic carbonates, Beilstein J. Org. Chem. 12 (2016) 1911–1924.

[48] Z.I. Ishak, N.A. Sairi, Y. Alias, M.K.T. Aroua, R. Yusoff, A review of ionic liquids as catalysts for transesterification reactions of biodiesel and glycerol carbonate production, Catal Rev 59 (1) (2017) 44–93.

[49] Z.I. Ishak, N.A. Sairi, Y. Alias, M.K.T. Aroua, R. Yusoff, Production of glycerol carbonate from glycerol with aid of ionic liquid as catalyst, Chem. Eng. J. 297 (2016) 128–138.

[50] R. Lambert, P. Coupillaud, A.-L. Wirotius, J. Vignolle, D. Taton, Imidazolium-Based Poly(Ionic Liquid)s Featuring Acetate Counter Anions: Thermally Latent and Recyclable Precursors of Polymer-Supported N-Heterocyclic Carbenes for Organocatalysis, Macromol. Rapid Commun. 37 (14) (2016) 1143–1149.

[51] P. Stiernet, A. Aqil, X. Zhu, A. Debuigne, Multicomponent Radziszewski Emulsion Polymerization toward Macroporous Poly(ionic liquid) Catalysts, ACS Macro Lett. 9 (1) (2020) 134–139.

Published in : European Polymer Journal (2021), vol. 147, n°110296
DOI: 10.1016/j.eurpolymj.2021.110296
Status : Postprint (Author's version)

[52] D. Esposito, S. Kirchhecker, M. Antonietti, A Sustainable Route towards Imidazolium Building Blocks Based on Biomass Molecules, Chem. Eur. J. 19 (45) (2013) 15097–15100.

[53] L. Matějka, S. Pokomý, K. Dušek, Network formation involving epoxide and carboxyl groups, Polym. Bull. 7 (2) (1982) 123–128.

[54] M. Kumar, S. Bagchi, A. Sharma, The first vinyl acetate mediated organocatalytic transesterification of phenols: a step towards sustainability, New J. Chem. 39 (11) (2015) 8329–8336.

[55] X. Niu, F. Wang, X. Li, R. Zhang, Q. Wu, P. Sun, Using Zn2+ Ionomer To Catalyze Transesterification Reaction in Epoxy Vitrimer, Ind. Eng. Chem. Res. 58 (14) 5698–5706.

[56] X. Wu, X. Yang, R. Yu, X.-J. Zhao, Y. Zhang, W. Huang, A facile access to stiff epoxy vitrimers with excellent mechanical properties via siloxane equilibration, J. Mater. Chem. 6 (22) (2018) 10184–10188.

[57] Q. Shi, K. Yu, M.L. Dunn, T. Wang, H.J. Qi, Solvent Assisted Pressure-Free Surface Welding and Reprocessing of Malleable Epoxy Polymers, Macromolecules 49 (15) (2016) 5527–5537.